

Neural basis of 3-D shape aftereffects

Andrea Li^{a,*}, Belinda Tzen^a, Alevtina Yadgarova^a, Qasim Zaidi^b

^a Department of Psychology, Queens College, 65-30 Kissena Boulevard, Flushing, NY 11367, USA

^b Department of Vision Sciences, SUNY College of Optometry, 33 W 42nd Street, New York, NY 10036, USA

Received 27 April 2007; received in revised form 1 November 2007

Abstract

We used selective adaptation to identify the neural mechanisms responsible for 3-D shape perception from orientation flows in retinal images [Li, A., & Zaidi, Q. (2000). Perception of three-dimensional shape from texture is based on patterns of oriented energy. *Vision Research* 40 (2), 217–242]. Three-dimensional shape adaptation could involve stages from photoreceptors to non-oriented retinal cells, oriented cells in striate cortex, and extra-striate cells that respond to 3-D slants. To psychophysically isolate the relevant stage, we used 3-D adapting stimuli created from real and illusory orientations, and test stimuli different from the adapting stimuli in phases and frequencies. The results showed that mechanisms that adapt to 3-D shapes combine real and illusory 2-D orientation information over a range of spatial frequencies.

© 2007 Elsevier Ltd. All rights reserved.

Keywords: 3-D shape; Shape-from-texture; Adaptation; Orientation flows; Extra-striate neurons

1. Introduction

The perception of 3-D shape from static monocular cues such as shading and texture is effortless, but little is known about the underlying neural mechanisms. Although neurons in extra-striate areas AIT, the anterior infero-temporal lobe (Liu, Vogels, & Orban, 2004) and CIP, the caudal part of the lateral bank of intra-parietal sulcus (Tsutsui, Sakata, Naganuma, & Taira, 2002) have been shown to respond selectively to slants defined by monocular texture cues, the image features to which these cells respond have not been isolated. Similarly, fMRI studies of 3-D shape processing (Ishai, Ungerleider, Martin, Schouten, & Haxby, 1999; Kourtzi, Erb, Grodd, & Bulthoff, 2003; Kourtzi & Kanwisher, 2000, 2001; Sereno, Trinath, Augath, & Logothetis, 2002) have focused on localization of function rather than systematically isolating neural properties. Psychophysical experiments have shown that

the visibility of specific patterns of orientation flows determines the perception of 3-D shapes from texture cues (Knill, 2001; Li & Zaidi, 2000, 2004). When particular patterns of orientation flows are visible, observers invariably see the corresponding 3-D percepts. Since there is no way to separate the 2-D pattern and the 3-D percept, we assume that any neuron that responds selectively to one of the 2-D patterns will automatically signal the 3-D shape. Orientation flows have also been identified as critical to 3-D perception from shading and reflection cues (Breton & Zucker, 1996; Fleming, Torralba, & Adelson, 2004). The goal of the present study was to use selective adaptation to identify the properties of neural mechanisms that extract 3-D shape from orientation flows.

Selective adaptation seeks to identify a set of neural mechanisms whose responses span a stimulus dimension. In the past, adaptation has been used to identify mechanisms selective for stimulus properties like wavelength, color, orientation, spatial frequency, and velocity (e.g. Blakemore & Sutton, 1969; Sachtler & Zaidi, 1993; Stiles, 1959; Wade, 1970, 1994; Zaidi & Shapiro, 1993). The effect of prolonged exposure to each of a number of stimuli vary-

* Corresponding author.

E-mail address: Andrea.Li@qc.cuny.edu (A. Li).

ing along the stimulus dimension is assessed by measuring changes in sensitivity to, or appearance of, a wide range of stimuli varying along the dimension of interest. The results are modeled as changes in population responses. For example, if there are neural mechanisms that range in selectiveness from concave to convex 3-D curvatures, and each mechanism adapts proportionately to its activation, then adaptation to a convex surface should cause a flat surface to appear concave, and a flat percept would require a physically convex surface. The opposite results would be expected for adaptation to a concave surface. Signs of the aftereffects provide qualitative evidence for the selectivity of neural mechanisms, and shifts in the observer's perceived flat point along the concave–convex dimension provide quantitative measures of the strengths of the aftereffects which are then related to the sensitivities of the mechanisms.

Selective adaptation is often called the psychophysicist's micro-electrode, but no psychophysical adaptation procedure has been shown to have effects restricted to one stage of the visual system. In particular, prolonged exposure to 3-D shapes can lead to adaptation of photoreceptors, non-oriented ganglion and LGN cells, oriented cells in striate cortex, and 3D-shape selective cells in extra-striate cortex. To identify the properties of 3D-shape selective cells, we measured aftereffects from 3-D percepts due to illusory

as well as real tilts, on test stimuli of phases and frequencies different from as well as identical to the adapting stimuli. We use the results of this study to answer questions about the existence of 3-D shape-selective neurons that are selective for particular patterns of orientation flows, and properties of the processes by which orientation flows are extracted.

2. Experiment 1: Ruling out unoriented and independent oriented cells

The left panels of Fig. 1 show checkerboards warped to convey convex (top) and concave (bottom) curvatures. The edges of the checks form curved orientation flows. The panels on the right which are variations of Zabuton illusions (Kitaoka, Pinna, & Brelstaff, 2004), actually consist of flat, perfectly square checkerboards, with black and white star-like figures at the intersections. The top and bottom panels are identical except that the polarities of the stars are opposite. Hence the non-horizontal and non-vertical tilts are illusory. The illusory tilts form illusory orientation flows that convey convex and concave surfaces that curve towards and away from the observer as convincingly as do the physically curved orientation flows in the left panels. The illusory tilts cannot be computed from the unaltered outputs of local orientation-tuned neurons since

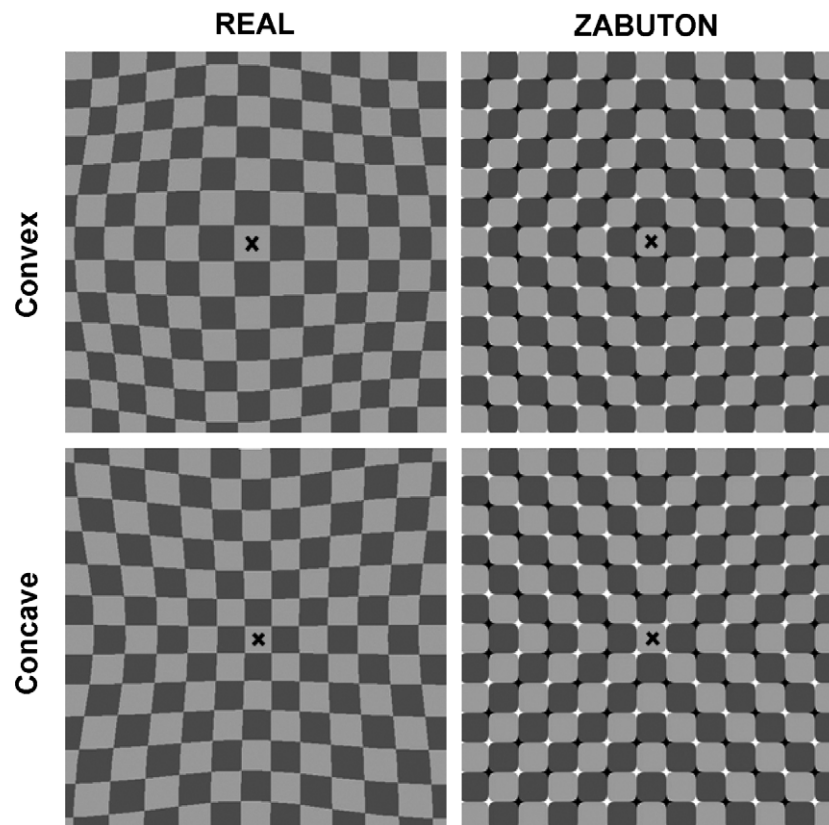


Fig. 1. Left panels: Three-dimensional convex and concave curvatures generated by warping checkerboards. Right panels: Zabutons consist of regular checkerboards containing black and white stars at intersections that induce illusory tilts of the edges and create illusory 3-D curvatures. Both sorts of images were used as adapting stimuli in Experiment 1.

these neurons would encode all edges as horizontal or vertical. Our first goal in Experiment 1 was to determine if neural mechanisms that code 3-D shape could be adapted as much by orientation flows composed of illusory tilts as by curvature-matched physically curved orientation flows (we refer to these physically curved flows as “real”). The second goal was to show that a sufficient explanation requires more than adaptation of unoriented neurons or oriented phase-sensitive V1 neurons that have small receptive fields.

2.1. Experimental procedures

2.1.1. Stimuli

There were four sets of adapting stimuli: Concave and convex Zabutons (Fig. 1, right), and concave and convex Real adapting stimuli (Fig. 1, left). Zabuton adapting stimuli were generated using Canvas and Adobe Photoshop. Real adapting stimuli were generated in MATLAB by warping a regular checkerboard pattern into a surface defined by the equation:

$$z = k \left[\cos x + \cos y + \frac{(\cos 3x + \cos 3y)}{3} \right] \quad (1)$$

where the value of k controlled the physical curvature (negative corresponding to concave, positive corresponding to convex). We used values of k that roughly equated physical curvature to the perceived curvature of the Zabuton, i.e. $k = -0.8$ for the concave adapting stimulus, and $k = +0.8$ for the convex adapting stimulus.

Test stimuli were images of checkerboard surfaces defined by Eq. (1). There were nine possible shapes ($k = -0.8, -0.4, -0.2, -0.1, 0, 0.1, 0.2, 0.4, \text{ and } 0.8$), and three possible phases of the checkerboard pattern for each shape: (1) *Same-phase*: The arrangement of the checks of the test and adapting stimulus were identical, thus contrasts of checks were almost but not perfectly retinally aligned. The misalignment was caused by edges of two stimuli of different curvatures having different local orientations and the spatial displacement increasing with eccentricity. (2) *Opposite-phase*: Checks of the test were contrast-reversed with respect to the adapting stimulus. (3) *Quadrature-phase*: Checks of the test were shifted horizontally and vertically by a quarter cycle (i.e. half a check).

In the main experiment, adapting and test stimuli subtended 6.5° (each check subtending 0.5°) and were presented on a background field with a mean luminance of 25 cd/m^2 . The Michelson contrast of the checks was 25%. We ran an additional “close” condition, where the viewing distance was halved so that the stimuli subtended 13° (each check subtending 1.0°).

2.1.2. Procedure

Before beginning the experiment, observers were presented with pictures of the Real concave and convex stimuli on a piece of paper. They were asked to describe what they saw in each picture in their own words. This was done to

insure that observers could in fact perceive different 3-D shapes from their 2-D representations. All observers correctly perceived the curvatures curving towards them (convex), and the curvatures curving away from them (concave).

Observers ran a total of 13 sessions each (1 baseline, 12 adaptation). Within each adaptation session, there was a single adapting stimulus (e.g. concave Zabuton), and each of the 27 test images was presented three times, randomly interleaved, for a total of 81 trials. Each adaptation session was then repeated two more times to acquire a total of 9 measurements for each of the 27 test images.

Each of the adaptation sessions began with a 1 min adaptation to the background mean luminance with a central fixation point that remained on the screen for the duration of the session. This was followed by 2 min of initial adaptation to one of the four adaptation stimuli. A brief 200 ms inter-stimulus interval consisting of the grey background was followed by one of the 27 test stimuli, presented for 200 ms. A beep coincided with the onset of the test stimulus. The test stimulus was followed by a 400 ms Gaussian noise mask intended to remove any aftereffects of the test stimuli. After the mask, the screen returned to the mean grey until the observer made a response. Observers were asked to report the shape of the test stimulus as either curving towards or away from them using a response box. In subsequent trials, a 5 s adapting stimulus was presented before each test stimulus in order to maintain the level of adaptation throughout the session. Each session lasted approximately 15 min.

A baseline session was run before the adaptation sessions to determine shape percepts prior to adaptation. Each of the 27 test stimuli was presented 9 times in a single session that lasted approximately 10 min. Observers practiced baseline and adaptation conditions before the actual experiment to become familiar with the task.

2.1.3. Apparatus and presentation

All stimuli were saved in Bitmap form and presented on a 22” Mitsubishi Diamond Pro 2070 flat screen CRT monitor with an 800×600 pixel screen running at a refresh rate of 80 frames/s via a Cambridge Research Systems ViSaGe Visual Stimulus Generator controlled through a 3.2 GHz Pentium 4 PC. Experimental code was written using the CRS Toolbox for MATLAB. Observers used the CRS CB6 infrared response box to make responses.

Observers’ head positions were fixed in a chin-rest situated 122 cm away from the stimulus monitor. All stimuli were presented centered on the screen so that the center of each image was level with the observer’s eye-height. Viewing was monocular in a dimly lit room, and there was no feedback. To minimize fatigue, observers typically ran no more than three adaptation sessions in one day (with short breaks in between). The order in which the adaptation conditions were run was randomized within and across observers.

2.1.4. Observers

Two of the authors and four naïve observers participated in the main experiment. Two of the observers from the original experiment and one new naïve observer participated in the “close” condition. All had normal or corrected-to-normal acuity. The naïve observers received course credit for their participation.

2.2. Results

2.2.1. Analysis

For each observer, 15 sets of data were obtained (4 adaptation and 1 baseline condition for each of 3 phases). For each set, the percentage of trials reported as convex was plotted vs. the curvature of the test shape quantified by the value of k in Eq. (1). A least-squares procedure was used to fit Weibull functions to each data set. As an example, Fig. 2 shows data from one observer for the baseline and four adaptation sessions for the Opposite-phase tests. Subjectively flat stimuli were estimated from the fits to each of the 15 data sets as the curvature (k) that would yield convex responses on half of the trials. If there was no effect of adaptation, the subjectively flat stimuli in the adaptation conditions would not differ from the baseline condition. A negative aftereffect from adapting to a convex surface causes a flat ($k = 0$) surface to appear concave, and the entire psychometric function to shift away from the baseline curve towards the right (e.g., solid symbols in Fig. 2). Thus the subjectively flat stimulus corresponds to a physically convex surface. Conversely, a negative aftereffect from adapting to a concave surface (e.g., open symbols in Fig. 2) causes a flat surface to appear convex, the entire

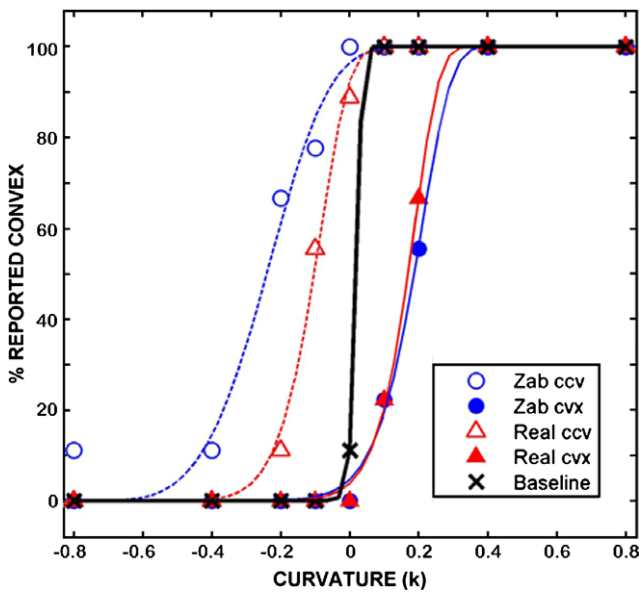


Fig. 2. Psychometric curves from Experiment 1 for one observer for the Opposite-phase test condition. Different symbols represent different adapting conditions. Data were fit with Weibull functions and subjectively flat curvatures were extracted as the values of k which would yield convex responses on 50% of the trials.

psychometric curve to shift towards the left, and the subjectively flat curvature to correspond to a physically concave surface. Positive aftereffects would cause opposite shifts.

Fig. 3 summarizes estimates of subjectively flat curvatures averaged across six observers for each of the three test phases. Error bars represent 95% confidence intervals. Subjectively flat stimuli in the baseline sessions were not significantly different from physically flat stimuli and so these

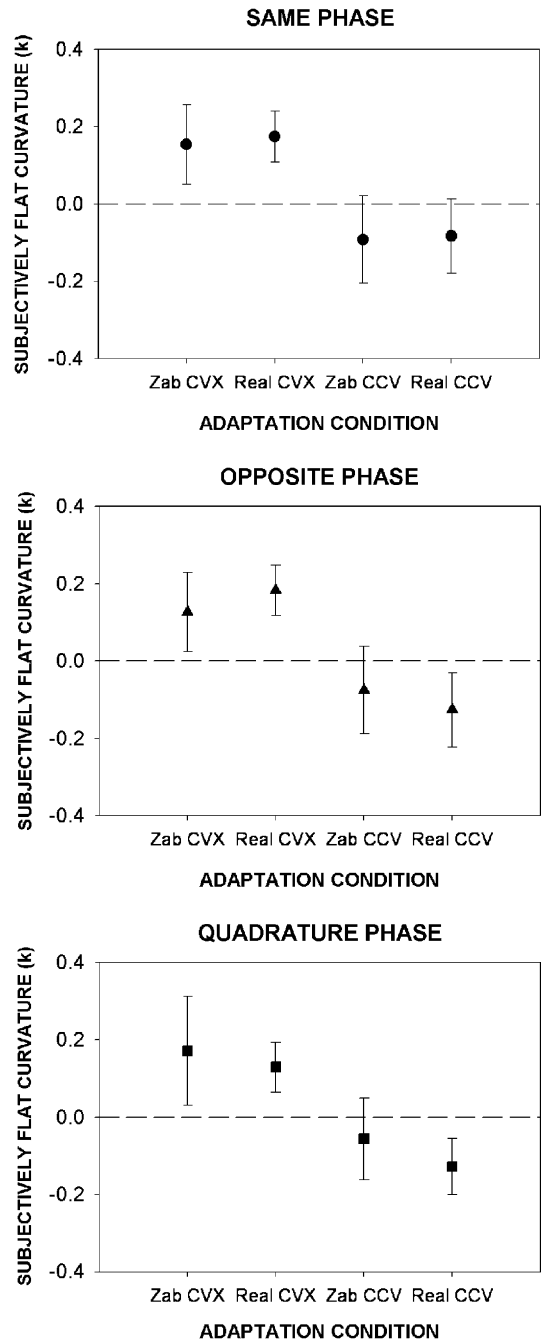


Fig. 3. Subjectively flat curvatures for Experiment 1 for each test phase after adapting to stimuli on the abscissa, averaged across six observers. Negative values on the ordinate represent concave shapes, positive represent convex shapes. Error bars represent 95% confidence intervals.

data are not shown. Adaptation to the Zabutons leads to aftereffects with signs and magnitudes similar to those from the curvature matched real flows. Results for all three phases of tests show a similar pattern: Adaptation to convex stimuli results in a shift of the subjectively flat curvature towards positive (convex) values. The converse is true for adaptation to a concave stimulus; the subjectively flat curvature shifts towards negative (concave) values. Unlike for convex adapting stimuli, the magnitude of concavity required for flat percepts after adapting to concave stimuli was less likely to be reliably different from physically flat. However, summarized over the six observers, 22/24 of the subjectively flat curvatures were shifted in the correct direction away from zero, for each of the three test phase conditions. The difference between the concave and convex results suggests that 3-D curvature adaptation may not be reduced to adaptation to individual 3-D slants.

2.3. Discussion

Below we compare the measured aftereffects from the three different test conditions to predictions from adaptation of possible neural mechanisms at different stages of the visual system.

To simulate adaptation of punctate unoriented luminance mechanisms to a Zabuton, the predicted percept (p) was computed by applying a point-by-point gain (Hayhoe, Benimoff, & Hood, 1987; Zaidi, Shapiro, & Hood, 1992) to the test stimulus (s):

$$p = \frac{j}{j+a} * s \quad (2)$$

where j is a gain constant and a is the local luminance of the adapting stimulus. The predicted percepts of a flat checkerboard after adaptation to a concave Zabuton for $j = 0.33$ are shown in Fig. 4 for each of the three test phases. (The value of 0.33 was chosen arbitrarily. A large range of values gives qualitatively similar results). A convex negative aftereffect is predicted for the Same-phase condition, a concave positive aftereffect for the Opposite-phase condition, and no curvature aftereffect for the Quadrature-phase condition. The results clearly rule out these

predictions. Similar predictions would be made for unoriented local contrast adaptation, thus adaptation of unoriented cells can not explain the shape aftereffects.

Adaptation of local orientation-tuned neurons such as those found in V1 (Blakemore & Campbell, 1969; Blakemore, Carpenter, & Georgeson, 1970; Carpenter & Blakemore, 1973) to real edges that are tilted clockwise from vertical will depress the population response around these stimulus orientations and thus cause a subsequently presented vertical edge to appear tilted counter-clockwise. As a result, adapting to a real convex image will cause the horizontal and vertical edges of a subsequently viewed flat checkerboard to appear tilted in configurations similar to those of a concave image. Thus negative aftereffects would not require higher level 3-D shape-selective mechanisms. However, the V1 neurons that would respond best to the edges in the Zabutons are those that are selective for horizontal and vertical orientations, and should not result in shape aftereffects for any of the three test phases. The Zabuton adaptation results thus rule out such neurons.

The next possibility is adaptation of orientation-selective neurons that respond to the illusory tilts, i.e. neurons whose responses are modified by the surrounding stars. A

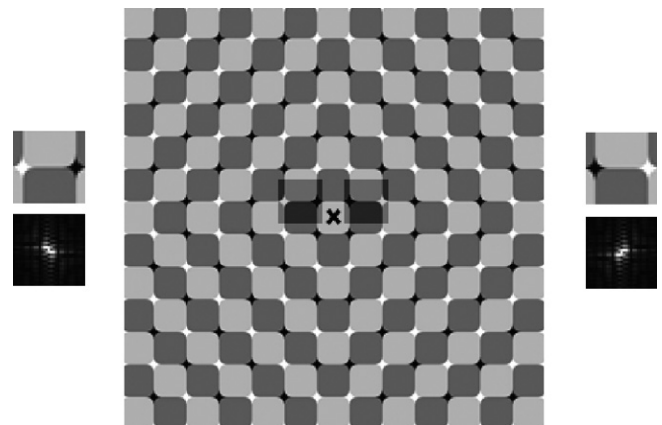


Fig. 5. Local Fourier spectra of segments bounded by two adjacent stars in the Zabuton exhibit energy oriented in the same directions as the illusory tilts.

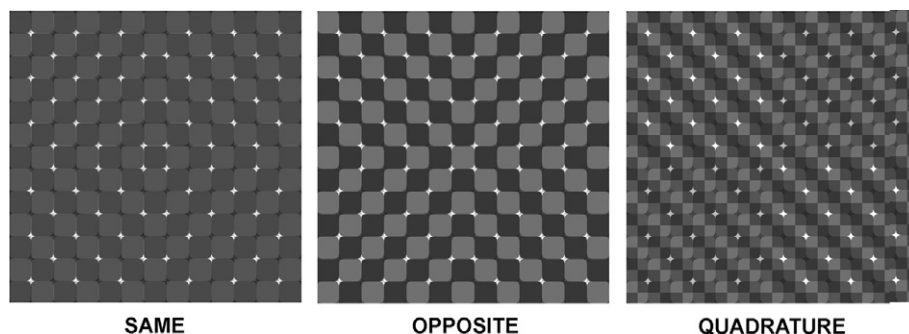


Fig. 4. Simulated percepts resulting from local luminance adaptation to a concave Zabuton on three flat checkerboard tests at each of the three test phases. Adaptation results in a negative shape aftereffect for the Same-phase test, a positive shape aftereffect for the Opposite-phase test, and no shape aftereffect for the Quadrature-phase test.

clue to the sorts of neurons that could lead to the illusory tilts in the Zabutons is provided by graphing the Fourier energy in segments bounded by two adjacent stars. Fig. 5 shows that these segments contain energy oriented in the same directions as the illusory tilts, but at very low frequencies. In order for an oriented neuron to extract this energy, it would have to be sensitive to the contrast polarity of the stars since this dictates the axis of the oriented energy. In addition, our results show that reversing the contrast in the Opposite-phase condition and shifting the test edges from the adapting edges in the Quadrature-phase condition had no effect on the aftereffect magnitudes. Thus, the required oriented neurons would also have to be insensitive to the contrast and spatial alignment of the checks, otherwise the strongest aftereffects would occur when the phase of the test checkerboard is matched to the phase of the adapting stimulus, and aftereffects would weaken as the retinal positions of the edges in the test and the edges in the adapting stimulus are progressively misaligned. To summarize, we need the adapting cells to be simultaneously sensitive to the phase of the Zabuton stars and insensitive to the phase of the checks. In addition these neurons would have to dominate the response to the test stimulus at some stage of the visual system, otherwise unadapted responses of other sorts of neurons would lead to lack of aftereffects. These considerations rule out not only conventionally defined simple and complex cells, but also the much sparser V1 cells that do respond to complex patterns (Victor, Mechler, Repucci, Purpura, & Sharpee, 2006). Single cell electrophysiology and optical imaging studies have found V1/V2 cells that respond to illusory contours (Ramsden, Hung, & Roe, 2001; von der Heydt & Peterhans, 1989), and psychophysical and fMRI studies have found selectivity for and adaptation to illusory contours (Mendola, Dale, Fischl, Liu, & Tootell, 1999; Montaser-Kouhsari, Landy, Heeger, & Larsson, 2007; Paradiso, Shimojo, & Nakayama, 1989), however it is not clear to us whether the cells identified by these methods would respond to illusory tilts in the Zabutons which contain solid, luminance-defined contours while conventional illusory contours do not.

An additional clue which may help further characterize the neurons required to extract the illusory tilts comes from a control condition in which the stimulus was enlarged to twice the size by reducing the viewing distance. Since each check in the original patterns spanned 0.5° , edges in the adapting and test stimuli were misaligned by 0.25° in the Quadrature-phase conditions. Simple cells could still contribute to aftereffects with this misalignment if ON/OFF regions of simple cells spanned up to 0.5° in the direction orthogonal to the preferred orientation. To more definitively rule out contributions of simple cells, we ran three observers in the same experiment with a reduced viewing distance such that each check spanned 1.0° . The Zabuton illusions at this distance were still apparent. Subjectively flat curvatures for the enlarged stimulus condition averaged across three observers are plotted in Fig. 6 in the same format as Fig. 3. Aftereffects were obtained in all condi-

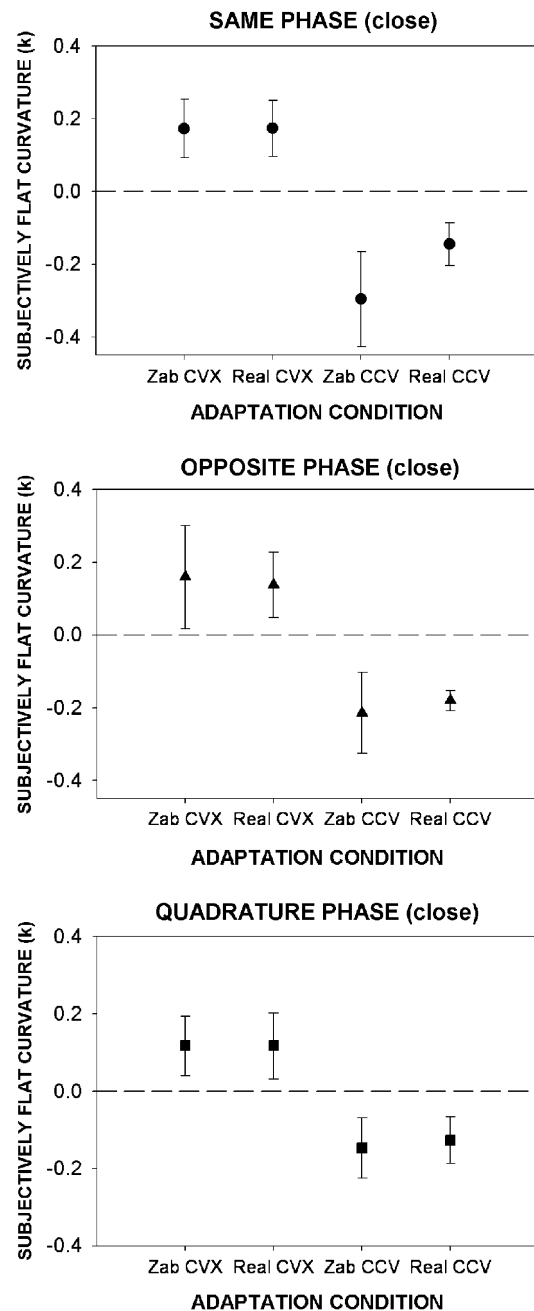


Fig. 6. Subjectively flat curvatures for Experiment 1 measured for the “close” stimulus condition in which each check was doubled in size to 1° , averaged across three observers, plotted in the same format as in Fig. 3. Error bars represent 95% confidence intervals.

tions, and subjectively flat curvatures for concave/convex and real/Zabuton adapting stimuli were reliably different from physical flatness. For each of the three test phase conditions, tallied across the three observers, 12/12 of the subjectively flat curvatures were shifted in the direction away from zero consistent with a negative aftereffect. Although there is some variability in receptive field size across cortical layers, physiological studies have shown that more than half of V1 cells within 5° of the fovea have receptive field diameters of less than 1° , with a majority of receptive fields

spanning less than 2° (Cavanaugh, Bair, & Movshon, 2002, Fig. 2). This roughly translates to ON/OFF regions spanning no more than $0.5\text{--}1^\circ$. Thus aftereffects obtained in the enlarged Quadrature-phase Zabuton conditions would likely result from adaptation of other mechanisms, presumably with ON/OFF regions greater than 1.0° .

3. Experiment 2: Ruling out frequency-limited cells

To examine the frequency selectivity of the neural mechanisms involved in 3-D shape adaptation, we exploited the finding that tuning curves of V1 (and most V2) neurons in the fovea average a frequency range between 2.6 and 3.0 (Foster, Gaska, Nagler, & Pollen, 1985). This is reflected in the essential absence of psychophysical contrast adaptation when test and adapting frequencies differ by a factor of two (Blakemore & Campbell, 1969; Blakemore, Nachmias, & Sutton, 1970). Thus if these cells were being adapted, we would not expect to see shape aftereffects when the test pattern frequencies differed by more than a factor of two from the adapting frequencies.

In Experiment 2, we used images of sinusoidal corrugations, each patterned with a horizontal–vertical sinusoidal plaid of either 2 or 6 cpd (Fig. 7). These frequencies were chosen to differ by a factor of three while remaining within the range that conveys correct 3-D shape for these corrugations. Each image subtended 6.5° and contained 1.5 cycles

of the corrugation, centered on either a concavity or a convexity. Adapting corrugations had simulated peak-to-trough amplitude equal to 14 cm for a surface viewed at 100 cm. There were nine possible test shapes: Curvatures identical in amplitude to the two adapting stimuli, and seven additional corrugations at intermediate amplitudes ($-14, -10.5, -6.5, -2.5, 0, 2.5, 6.5, 10.5, \text{ and } 14$ cm). For each shape, the plaid was mapped as the surface of a carved solid (Li & Zaidi, 2004) at one of two different random phases. This resulted in a total of 18 different test images (9 shapes \times 2 plaid phases) each of which was presented randomly three times for a total of 54 trials per session. All other aspects of Experiment 2 were identical to those of Experiment 1. Each adaptation session was run twice to yield 12 measurements for each of the 18 test shapes. One of the authors and six naïve observers participated. All had normal or corrected-to-normal acuity.

Results between the two phases did not differ significantly, and were averaged. Fig. 8 shows the subjectively flat curvatures averaged across six different observers separately for the high and low frequency adapting patterns (2 and 6 cpd). Within each panel, mean subjectively flat curvatures are plotted for each of the test conditions grouped by pattern frequency and 3-D curvature. Error bars represent 95% confidence intervals. The results show aftereffects for within and across adapting and test frequencies. For the high and low frequency adapting stimuli, 23/

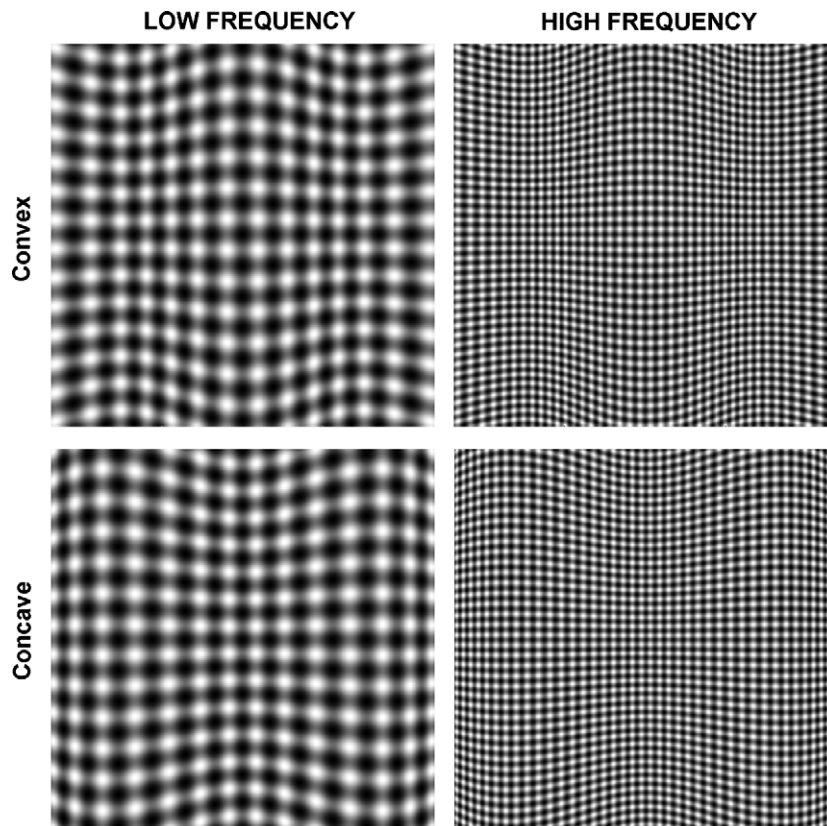


Fig. 7. Adapting stimuli used in Experiment 2. Sinusoidally corrugated carved solids textured with either 2 or 6 cpd horizontal–vertical plaid patterns. Images contained 1.5 cycles of corrugations that were either centrally convex or concave.

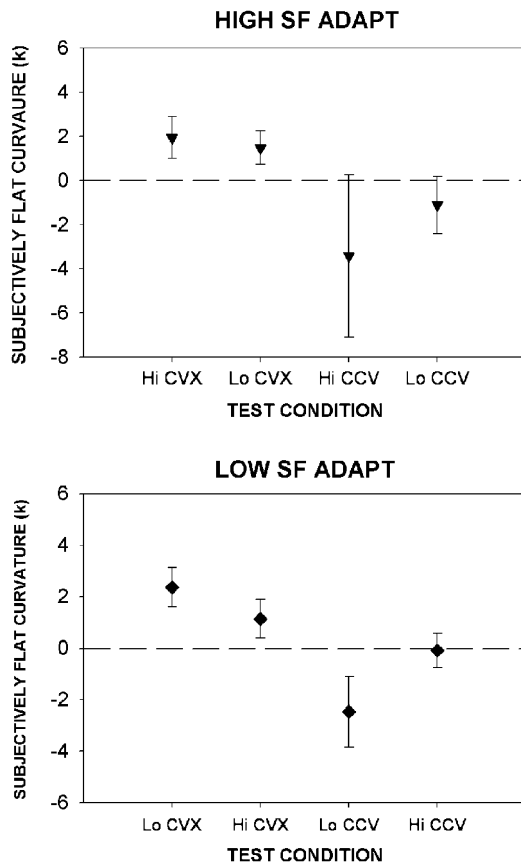


Fig. 8. Subjectively flat curvatures for Experiment 2 plotted for the high and low frequency test stimuli across the four adaptation stimuli, averaged across six observers. Error bars represent 95% confidence intervals.

24 and 22/24 of the subjectively flat curvatures were shifted away from zero in the right direction. The two leftmost points in both panels show that adaptation to convex stimuli of the same or opposite frequency reliably shifted subjectively flat curvatures towards convex values. The two rightmost points in both panels show that adaptation to a concave stimulus resulted in reliable aftereffects only when the frequencies of the adapting and test patterns were low. Thus reliable aftereffects were obtained in two out of the four conditions in which the adapting and testing frequencies differed by a factor of three. That in three out of the four cross-adaptation conditions, the means were shifted in the correct direction away from zero indicates that adaptation is occurring in cells that are more broadly tuned for spatial frequency than are V1, and most V2, neurons.

4. Conclusion

The results of Experiments 1 and 2 rule out V1 and V2 as primary sites of 3-D shape aftereffects from adaptation to orientation flows. The most parsimonious interpretation of our results is that adaptation is taking place at the level of neurons that respond selectively to 3-D curvatures or tilts. In psychophysical experiments, there

is a one-to-one relationship between 3-D percepts and the visibility of the corresponding 2-D orientation flows, therefore Zaidi and Li (2002) proposed models for 3-D shape selective neurons in which responses of neurons to 3-D shapes are proportional to the matches between the orientation flows in the images and templates for orientation flows corresponding to shapes of particular curvature and orientation. The response of the visual system to a 3-D shape then is calculated from the population responses of such neurons. The results of this study indicate that these models need to be supplemented in a number of ways. First, such neurons should respond equally well to shifted patterns of 2-D orientation flows as long as the image of their preferred slant or curvature falls within their receptive fields. Second, the response to the 3-D stimulus should be invariant to the contrast polarity and spatial frequency of the flows. Third, the orientation flows can have real or illusory curvature. Further support that our experiments have isolated the adaptation of such neurons comes from informal observations that adapting to the orientation flows of surfaces carved from horizontal-vertical plaid textured solids does not lead to 3-D aftereffects on frequency-matched flat textures that do not have strong orientation components, e.g. a random dot pattern. In macaque monkeys, the anterior infero-temporal lobe and caudal part of the lateral bank of intra-parietal sulcus have been shown to include neurons that are selective to 3-D surface orientation defined by texture cues (Liu et al., 2004; Tsutsui et al., 2002). For human brains, event-related fMRI has implicated both caudal and anterior areas of intra-parietal sulcus (Shikata et al., 2001; Welchman, Deubelius, Conrad, Bulthoff, & Kourtzi, 2005). When tested with 2-D shapes, many cells in infero-temporal lobe and intra-parietal sulcus have large receptive fields and are insensitive to position changes inside their receptive fields (Ito, Tamura, Fujita, & Tanaka, 1995). Our results suggest that these properties generalize to 2-D patterns of orientation flows that convey 3-D information. It remains to be seen whether they also generalize to the location of 3-D features.

Acknowledgments

This work was supported by PSC-CUNY Grants PSC-60066-35-36 and PSC-68149-00-37 to A. Li, and NIH EY13312 & EY07556 to Q. Zaidi, and was presented in parts at the Vision Sciences Society Meetings in Sarasota, Florida in May 2006 and 2007. The authors thank Diana Gerov and Albert Ilyayev for their help with the data collection.

References

- Blakemore, C., & Campbell, F. W. (1969). On the existence of neurons in the human visual system selectively sensitive to the orientation and size of retinal images. *Journal of Physiology*, 203(1), 237–260.

- Blakemore, C., Carpenter, R. H., & Georgeson, M. A. (1970). Lateral inhibition between orientation detectors in the human visual system. *Nature*, 228(5266), 37–39.
- Blakemore, C., Nachmias, J., & Sutton, P. (1970). The perceived spatial frequency shift: Evidence for frequency-selective neurons in the human brain. *Journal of Physiology*, 210(3), 727–750.
- Blakemore, C., & Sutton, P. (1969). Size adaptation: A new aftereffect. *Science*, 166(902), 245–247.
- Bretton, P., & Zucker, S. (1996). Shadows and shading flow fields. IEEE Conf. on Computer Vision and Pattern Recognition, 782–789.
- Carpenter, R. H., & Blakemore, C. (1973). Interactions between orientations in human vision. *Experimental Brain Research*, 18(3), 287–303.
- Cavanaugh, J. R., Bair, W., & Movshon, J. A. (2002). Nature and interaction of signals from the receptive field center and surround in macaque V1 neurons. *Journal of Neurophysiology*, 88(5), 2530–2546.
- Fleming, R. W., Torralba, A., & Adelson, E. H. (2004). Specular reflections and the perception of shape. *Journal of Vision*, 4(9), 798–820.
- Foster, K. H., Gaska, J. P., Nagler, M., & Pollen, D. A. (1985). Spatial and temporal frequency selectivity of neurones in visual cortical areas V1 and V2 of the macaque monkey. *Journal of Physiology*, 365, 331–363.
- Hayhoe, M. M., Benimoff, N. I., & Hood, D. C. (1987). The time-course of multiplicative and subtractive adaptation process. *Vision Research*, 27(11), 1981–1996.
- Ishai, A., Ungerleider, L. G., Martin, A., Schouten, J. L., & Haxby, J. V. (1999). Distributed representation of objects in the human ventral visual pathway. *Proceedings of the National Academy of Science of the United States of America*, 96(16), 9379–9384.
- Ito, M., Tamura, H., Fujita, I., & Tanaka, K. (1995). Size and position invariance of neuronal responses in monkey inferotemporal cortex. *Journal of Neurophysiology*, 73(1), 218–226.
- Kitaoka, A., Pinna, B., & Brelstaff, G. (2004). Contrast polarities determine the direction of Cafe Wall tilts. *Perception*, 33(1), 11–20.
- Knill, D. C. (2001). Contour into texture: Information content of surface contours and texture flow. *Journal of the Optical Society of America A*, 18(1), 12–35.
- Kourtzi, Z., Erb, M., Grodd, W., & Bulthoff, H. H. (2003). Representation of the perceived 3-D object shape in the human lateral occipital complex. *Cerebral Cortex*, 13(9), 911–920.
- Kourtzi, Z., & Kanwisher, N. (2000). Cortical regions involved in perceiving object shape. *Journal of Neuroscience*, 20(9), 3310–3318.
- Kourtzi, Z., & Kanwisher, N. (2001). Representation of perceived object shape by the human lateral occipital complex. *Science*, 293(5534), 1506–1509.
- Li, A., & Zaidi, Q. (2000). Perception of three-dimensional shape from texture is based on patterns of oriented energy. *Vision Research*, 40(2), 217–242.
- Li, A., & Zaidi, Q. (2004). Three-dimensional shape from non-homogeneous textures: Carved and stretched surfaces. *Journal of Vision*, 4(10), 860–878.
- Liu, Y., Vogels, R., & Orban, G. A. (2004). Convergence of depth from texture and depth from disparity in macaque inferior temporal cortex. *Journal of Neuroscience*, 24(15), 3795–3800.
- Mendola, J. D., Dale, A. M., Fischl, B., Liu, A. K., & Tootell, R. B. (1999). The representation of illusory and real contours in human cortical visual areas revealed by functional magnetic resonance imaging. *Journal of Neuroscience*, 19(19), 8560–8572.
- Montaser-Kouhsari, L., Landy, M. S., Heeger, D. J., & Larsson, J. (2007). Orientation-selective adaptation to illusory contours in human visual cortex. *Journal of Neuroscience*, 27(9), 2186–2195.
- Paradiso, M. A., Shimojo, S., & Nakayama, K. (1989). Subjective contours, tilt aftereffects, and visual cortical organization. *Vision Research*, 29(9), 1205–1213.
- Ramsden, B. M., Hung, C. P., & Roe, A. W. (2001). Real and illusory contour processing in area V1 of the primate: A cortical balancing act. *Cerebral Cortex*, 11(7), 648–665.
- Sachtler, W. L., & Zaidi, Q. (1993). Effect of spatial configuration on motion aftereffects. *Journal of the Optical Society of America A*, 10(7), 1433–1449.
- Sereno, M. E., Trinath, T., Augath, M., & Logothetis, N. K. (2002). Three-dimensional shape representation in monkey cortex. *Neuron*, 33(4), 635–652.
- Shikata, E., Hamzei, F., Glauche, V., Knab, R., Dettmers, C., & Weiller, C. (2001). Surface orientation discrimination activates caudal and anterior intraparietal sulcus in humans: An event-related fMRI study. *Journal of Neurophysiology*, 85(3), 1309–1314.
- Stiles, W. S. (1959). Colour vision: The approach through increment threshold sensitivity. *Proceedings of the National Academy of Science of the United States of America*, 45, 100–114.
- Tsutsui, K., Sakata, H., Naganuma, T., & Taira, M. (2002). Neural correlates for perception of 3D surface orientation from texture gradient. *Science*, 298(5592), 409–412.
- Victor, J. D., Mechler, F., Repucci, M. A., Purpura, K. P., & Sharpee, T. (2006). Responses of V1 neurons to two-dimensional hermite functions. *Journal of Neurophysiology*, 95(1), 379–400.
- von der Heydt, R., & Peterhans, E. (1989). Mechanisms of contour perception in monkey visual cortex. I. Lines of pattern discontinuity. *Journal of Neuroscience*, 9, 1731–1748.
- Wade, N. J. (1970). Effect of prolonged tilt on visual orientation. *The Quarterly Journal of Experimental Psychology*, 22(3), 423–439.
- Wade, N. J. (1994). A selective history of the study of visual motion aftereffects. *Perception*, 23(10), 1111–1134.
- Welchman, A. E., Deubelius, A., Conrad, V., Bulthoff, H. H., & Kourtzi, Z. (2005). 3D shape perception from combined depth cues in human visual cortex. *Nature Neuroscience*, 8(6), 820–827.
- Zaidi, Q., & Li, A. (2002). Limitations on shape information provided by texture cues. *Vision Research*, 42(7), 815–835.
- Zaidi, Q., Shapiro, A., & Hood, D. (1992). The effect of adaptation on the differential sensitivity of the S-cone color system. *Vision Research*, 32(7), 1297–1318.
- Zaidi, Q., & Shapiro, A. G. (1993). Adaptive orthogonalization of opponent-color signals. *Biological Cybernetics*, 69(5–6), 415–428.